Available online at www.sciencedirect.com
SCIENCE DIRECT®
Progress in Particle and Nuclear Physics 53 (2004) 225–237
Progress in Particle and Nuclear Physics
www.elsevier.com/locate/ppnp

Review

Strangeness dynamics in relativistic nucleus–nucleus collisions

E.L. Bratkovskaya[a], M. Bleicher[a], W. Cassing[b,*], M. van Leeuwen[c,d], M. Reiter[a], S. Soff[a], H. Stöcker[a], H. Weber[a]

[a] *Institut für Theoretische Physik, J.W. Goethe Universität, Robert-Mayer-Str. 8-10, D-60054 Frankfurt, Germany*
[b] *Institut für Theoretische Physik, Justus-Liebig Universität, Heinrich-Buff-Ring 16, D-35392 Giessen, Germany*
[c] *NIKHEF, Amsterdam, Netherlands*
[d] *Lawrence Berkely National Laboratory, Berkely, CA 94720, USA*

Abstract

We investigate hadron production as well as transverse hadron spectra in nucleus–nucleus collisions from 2 A GeV to 21.3 A TeV within two independent transport approaches (UrQMD and HSD) that are based on quark, diquark, string and hadronic degrees of freedom. The comparison to experimental data demonstrates that the two approaches agree quite well with each other and with the experimental data on hadron production. The enhancement of pion production in central Au+Au (Pb+Pb) collisions relative to scaled pp collisions (the 'kink') is well described by both approaches without involving any phase transition. However, the maximum in the K^+/π^+ ratio at 20 to 30 A GeV (the 'horn') is missed by ∼40%. A comparison to the transverse mass spectra from pp and C + C (or Si + Si) reactions shows the reliability of the transport models for light systems. For central Au + Au (Pb + Pb) collisions at bombarding energies above ∼5 A GeV, however, the measured $K^\pm$ m_T spectra have a larger inverse slope parameter than expected from the calculations. The approximately constant slope of the $K^\pm$ spectra at SPS (the 'step') is not reproduced either. Thus the pressure generated by hadronic interactions in the transport models above ∼5 A GeV is lower than observed in the experimental data. This finding suggests that the additional pressure—as expected from lattice QCD calculations at finite quark chemical potential and temperature—might be generated by strong interactions in the early pre-hadronic/partonic phase of central Au + Au (Pb + Pb) collisions.

PACS: 25.75.-q; 25.75.Dw; 13.60.Le; 12.38.Mh

Keywords: Relativistic heavy-ion collisions; Particle and resonance production; Meson production; Quark gluon plasma

* Corresponding author. Tel.: +49-641-993-3310; fax: +49-641-993-3309.
E-mail address: wolfgang.cassing@theo.physik.uni-giessen.de (W. Cassing).

0146-6410/$ - see front matter © 2004 Elsevier B.V. All rights reserved.
doi:10.1016/j.ppnp.2004.02.015

1. Introduction

The phase transition from partonic degrees of freedom (quarks and gluons) to interacting hadrons is a central topic of modern high energy physics. In order to understand the dynamics and relevant scales of this transition, laboratory experiments under controlled conditions are currently performed with ultrarelativistic nucleus–nucleus collisions. Hadronic spectra and relative hadron abundances from these experiments reflect important aspects of the dynamics in the hot and dense zone formed in the early phase of the reaction. Furthermore, as proposed early by Rafelski and Müller [1], the strangeness degree of freedom might play an important role in distinguishing hadronic and partonic dynamics.

In fact, estimates based on the Bjorken formula [2] for the energy density achieved in central Au + Au collisions suggest that the critical energy density for the formation of a quark–gluon plasma (QGP) is far exceeded during a few fm/c in the initial phase of the collision at relativistic heavy ion collider (RHIC) energies [3], but sufficient energy densities ($\sim$0.7–1 GeV/fm^3 [4]) might already be achieved at alternating gradient synchrotron (AGS) energies of $\sim$10 A GeV [5, 6]. More recently, lattice QCD calculations at finite temperature and quark chemical potential μ_q [7] showed a rapid increase of the thermodynamic pressure P with temperature above the critical temperature T_c for a phase transition to the QGP. The crucial question is, however, at what bombarding energies the conditions for the phase transition (or crossover) might be fulfilled.

Currently, transverse mass (or momentum) spectra of hadrons are at the center of interest. It is experimentally observed that the transverse mass spectra of kaons at AGS and SPS energies show a substantial *flattening* or *hardening* in central Au + Au collisions relative to pp interactions (cf. [8, 9]). In order to quantify this effect, the spectra are often parametrized as

$$\frac{1}{m_T}\frac{\mathrm{d}N}{\mathrm{d}m_T} \sim \exp\left(-\frac{m_T}{T}\right) \tag{1}$$

where $m_T = \sqrt{m^2 + p_T^2}$ is the transverse mass and T is the inverse slope parameter. This hardening of the spectra is commonly attributed to strong collective flow, which is absent in the pp or pA data.

The authors of [10, 11] have proposed to interprete the approximately constant $K^{\pm}$ slopes above $\sim$30 A GeV—the 'step'—as an indication of a phase transition, following an early suggestion by Van Hove [12]. This interpretation is also based on a rather sharp maximum in the K^+/π^+ ratio at $\sim$20 to 30 A GeV in central Au + Au (Pb + Pb) collisions (the 'horn' [10, 11]). However, it is currently not clear whether the statistical model assumptions invoked in [10, 11] hold reliably.

We will demonstrate in this contribution that the pressure needed to generate a large collective flow—to explain the hard slopes of the $K^{\pm}$ spectra as well as the 'horn' in the K^+/π^+ ratio—is not produced in the present models by the interactions of hadrons in the expansion phase of the hadronic fireball. In our studies we use two independent transport models that employ hadronic and string degrees of freedom, i.e., UrQMD (v. 1.3) [13, 14] and HSD [15, 16]. They take into account the formation and multiple rescattering of

hadrons and thus dynamically describe the generation of pressure in the hadronic expansion phase. This involves also interactions of 'leading' pre-hadrons that contain a valence quark (antiquark) from a primary 'hard' collision (cf. [15, 17]).

The UrQMD transport approach [13, 14] includes all baryonic resonances up to masses of 2 GeV as well as mesonic resonances up to 1.9 GeV as tabulated by the Particle Data Group [18]. For hadronic continuum excitations a string model is used with hadron formation times in the order of 1–2 fm/c depending on the momentum and energy of the hadron created. In the HSD approach, nucleons, Δ's, $N^*(1440)$, $N^*(1535)$, Λ, Σ and Σ^* hyperons, Ξ's, Ξ^*'s and Ω's as well as their antiparticles are included on the baryonic side whereas the 0^- and 1^- octet states are included in the mesonic sector. High energy inelastic hadron–hadron collisions in HSD are described by the FRITIOF string model [19] whereas low energy hadron–hadron collisions are modeled on the basis of experimental cross sections. Both transport approaches reproduce the nucleon–nucleon, meson–nucleon and meson–meson cross section data over a wide kinematic range. We point out that no explicit parton–parton scattering processes (beyond the interactions of 'leading' quarks/diquarks) are included in the studies below, contrary to the case for the multiphase transport model (AMPT) [20], which is currently employed from upper SPS to RHIC energies.

2. Hadron excitation functions and ratios

2.1. *pp versus central AA reactions—the 'kink'*

In order to explore the main physics from central AA reactions it is instructive to have a look at the various particle multiplicities relative to scaled pp collisions as a function of bombarding energy. With this aim we show in Fig. 1 the total multiplicities of π^+, K^+ and K^- (i.e., the 4π yields) from central Au + Au (at AGS) or Pb + Pb (at SPS) collisions (from UrQMD and HSD) in comparison to the scaled total multiplicities from pp collisions versus the kinetic energy per particle E_{lab}.

The general trends from the two transport approaches are quite similar: we observe a slight absorption of pions at lower bombarding energy and a relative enhancement of pion production by rescattering in heavy ion collisions above ∼10 A GeV. Kaons and antikaons from AA collisions are always enhanced in central reactions relative to scaled pp multiplicities, which is a consequence of strong final state interactions. Thus, the 'kink' in the pion ratio as well as the $K^{\pm}$ enhancement might result from conventional hadronic final state interactions.

2.2. *Particle yields in central collisions of heavy nuclei*

Fig. 2 shows the excitation function for π^+, π^-, K^+, K^- and $\Lambda + \Sigma^0$ yields (mid-rapidity (l.h.s.) and rapidity integrated (r.h.s)) from central Au + Au (Pb + Pb) collisions in comparison to the experimental data.[1] As can be seen from Fig. 2, the differences between the independent transport models are less than 20%. The maximum deviations between the models and the experimental data are less than ∼30%. In addition, a systematic analysis of

[1] Note that all data from the NA49 Collaboration at 30 A GeV have to be considered as 'preliminary'.

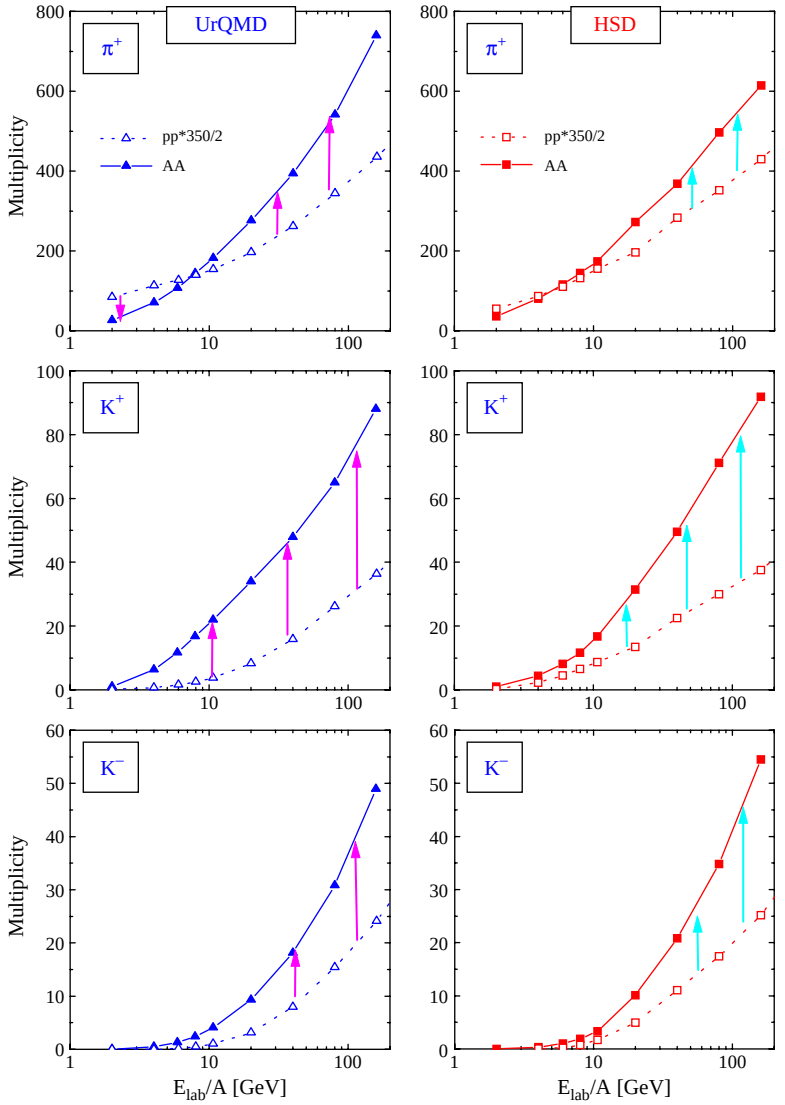

Fig. 1. Total multiplicities of π^+, K^+ and K^- (i.e., 4π yields) from central Au+Au (at AGS) or Pb+Pb (at SPS) collisions in comparison to the total multiplicities from pp collisions (scaled by a factor 350/2) versus kinetic energy E_{lab}. The solid lines with full triangles and squares show the UrQMD (l.h.s.) and HSD results (r.h.s.) for AA collisions, respectively. The dotted lines with open triangles and squares correspond to the pp multiplicities calculated within UrQMD (l.h.s.) and HSD (r.h.s.). The figure is taken from [17].

the results from both models and experimental data for central nucleus–nucleus collisions from 2 to 160 A GeV in [17] has shown that also the 'longitudinal' rapidity distributions of protons, pions, kaons, antikaons and hyperons are quite similar in the two models

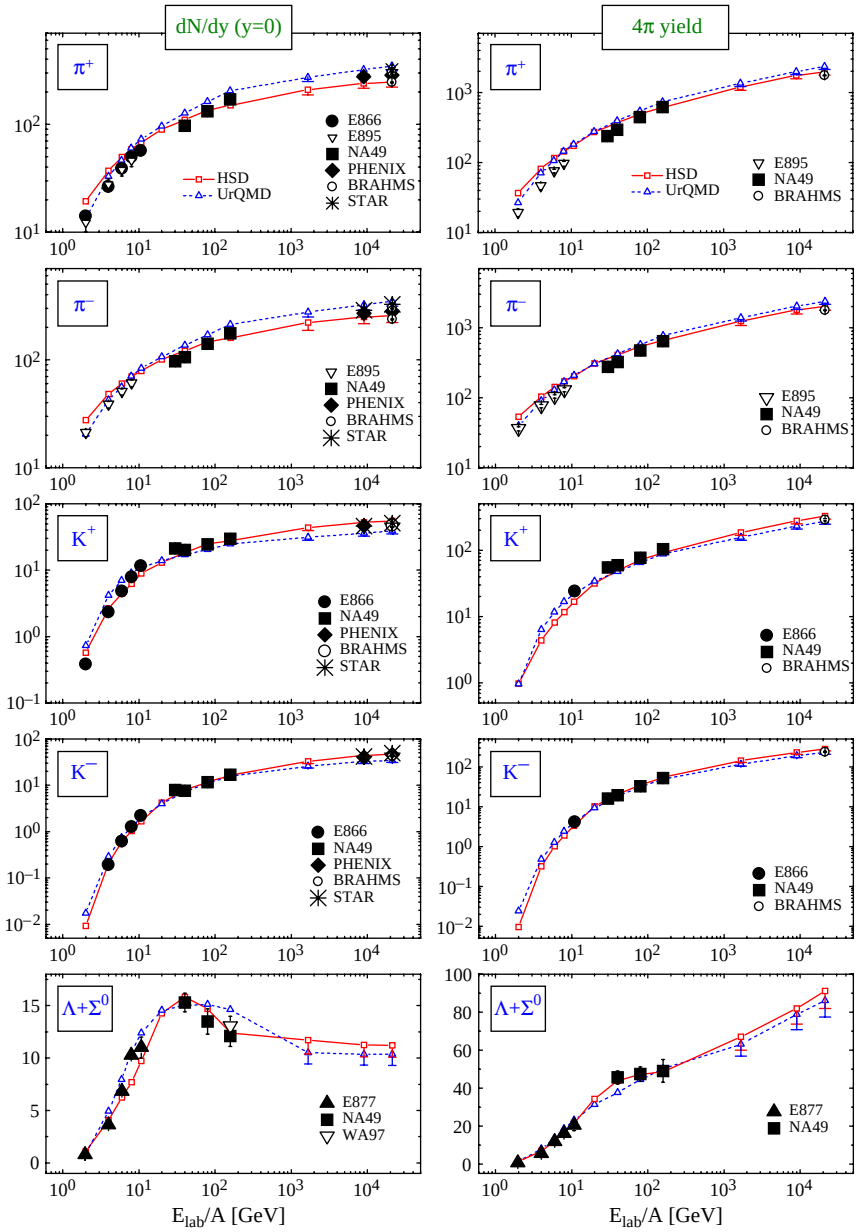

Fig. 2. The excitation function for π^+, π^-, K^+, K^- and $\Lambda + \Sigma^0$ yields from 5% central (AGS energies, SPS at 160 A GeV and at RHIC energies), 7% central (20, 30, 40 and 80 A GeV), 10% central for $\Lambda + \Sigma^0$ at 160 A GeV Au + Au (AGS and RHIC) or Pb + Pb (SPS) collisions in comparison to the experimental data from [21–23] (AGS), [24–26] (SPS) and [27–29] (RHIC) for mid-rapidity (left column) and rapidity integrated yields (right column). The solid lines with open squares show the results from HSD whereas the dashed lines with open triangles indicate the UrQMD calculations. The lower theoretical error bars at RHIC energies correspond to the yields for 10% central events. The figure is taken from [30].

and in reasonable agreement with available data. The exceptions are the pion rapidity spectra at the highest AGS energy and lower SPS energies, which are overestimated by both models [17]. For a more detailed comparison of HSD and UrQMD calculations with experimental data at RHIC energies we refer the reader to [31–33].

2.3. Particle ratios—the 'horn'

In Fig. 3 we present the excitation function for the particle ratios K^+/π^+, K^-/π^- and $(\Lambda+\Sigma^0)/\pi$ from central Au+Au (Pb+Pb) collisions in comparison to experimental data. The deviations between the transport models and the data are most pronounced for the mid-rapidity ratios (left column) since the ratios are very sensitive to actual rapidity spectra. The K^+/π^+ ratio in UrQMD shows a maximum at ∼8 A GeV and then drops to a constant ratio of 0.11 at top SPS and RHIC energies. In the case of HSD a continuously rising ratio with bombarding energy is found for the mid-rapidity ratios which is partly due to a dip in the pion pseudo-rapidity distribution at RHIC energies (cf. Fig. 1 in [31]). The 4π ratio in HSD is roughly constant from top SPS to RHIC energies; however, it is larger than the ratio from UrQMD due to the lower amount of pion production[2] and a slightly higher K^+ yield (cf. Fig. 2). Nevertheless, the experimental maximum in the K^+/π^+ ratio is missed, which we address dominantly to the excess of pions in the transport codes rather than to missing strangeness production. Qualitatively, the same arguments—due to strangeness conservation—also hold for the $(\Lambda+\Sigma^0)/\pi$ ratio, where the pronounced experimental maxima are underestimated due to the excess of pions in the transport models at top AGS energies (for HSD) and above ∼5 A GeV (for UrQMD). Since the K^- yields are well reproduced by both approaches (cf. Fig. 2) the deviations in the K^-/π^- ratios at SPS and RHIC energies in UrQMD can be traced back to the excess of pions (see the discussion above).

We stress that the maximum in the $(\Lambda+\Sigma^0)/\pi$ ratio is essentially due to a change from baryon to meson dominated dynamics with increasing bombarding energy. Similar arguments hold for the experimentally observed maxima in the ratio Ξ/π (cf. [34]). However, the 'horn' in the K^+/π^+ ratio at ∼30 A GeV is not described by either transport model.

3. Transverse mass spectra—the 'step'

We now focus on transverse mass spectra of pions and kaons/antikaons from central Au + Au (Pb + Pb) collisions from 2 A GeV to 21.3 A TeV and compare to recent data (cf. [35]). Without explicit representation we mention that the agreement between the transport calculations and the data for pp and for central C + C and Si + Si is quite satisfactory [35]; no obvious traces of 'new' physics are visible. The situation changes, however, for central Au + Au (or Pb + Pb) collisions. Whereas at the lowest energy of 4 A GeV the agreement between the transport approaches and the data is still acceptable, severe deviations are visible in the $K^\pm$ spectra at SPS energies of 30 and 160 A GeV [35].

[2] The lower amount of pions in HSD is essentially due to an energy-density cut of 1 GeV/fm^3, which prevents formation of hadrons above this critical energy density [17].

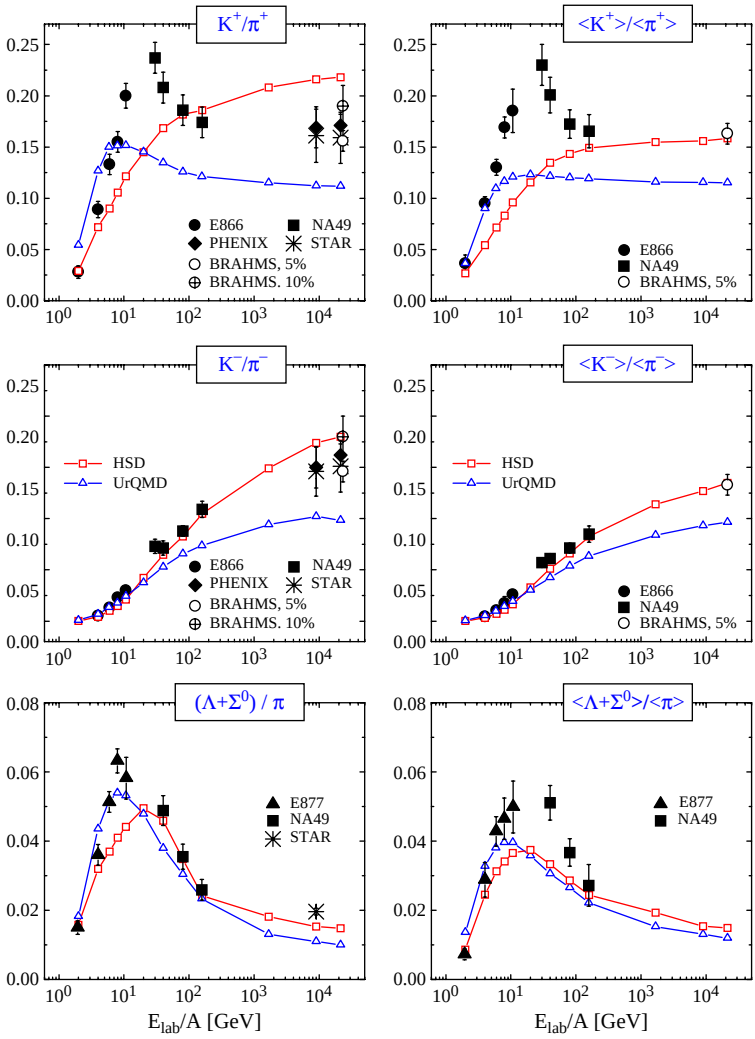

Fig. 3. The excitation function for K^+/π^+, K^-/π^- and $(\Lambda + \Sigma^0)/\pi$ ratios from 5% central (AGS energies, SPS at 160 A GeV and at RHIC energies), 7% central (20, 30, 40 and 80 A GeV), 10% central for $\Lambda + \Sigma^0$ at 160 A GeV Au + Au (AGS and RHIC) or Pb + Pb (SPS) collisions in comparison to the experimental data from [21, 23] (AGS), [24–26] (SPS) and [27–29] (RHIC) for mid-rapidity (left column) and rapidity integrated yields (right column). The solid lines with open squares show the results from HSD whereas the dashed lines with open triangles indicate the UrQMD calculations. The figure is taken from [30].

We note that the $\pi^{\pm}$ spectra are reasonably described at all energies while the inverse slope T of the $K^{\pm}$ transverse mass spectra in Eq. (1) is underestimated severely by about the same amount in both transport approaches (within statistics). The increase of the inverse $K^{\pm}$ slopes in heavy ion collisions with respect to pp collisions, which is generated by

rescatterings of the hadrons produced in the transport models, is small because the elastic meson–baryon scattering is strongly forward peaked and therefore gives little additional transverse momentum at mid-rapidity.

The question remains whether the underestimation of the $K^{\pm}$ slopes in the transverse mass spectra [35] might be due to conventional hadronic medium effects. In fact, the m_T slopes of kaons and antikaons at SIS energies (1.5–2 A GeV) were found to differ significantly [36]. As argued in [16], the different slopes could be traced back to repulsive kaon–nucleon potentials, which lead to a hardening of the K^+ spectra, and attractive antikaon–nucleon potentials, which lead to a softening of the K^- spectra. However, the effect of such potentials was calculated within HSD and found to be of minor importance at AGS and SPS energies [16] since the meson densities are comparable to or even larger than the baryon densities at AGS energies and above. Additional self-energy contributions stem from $K^{\pm}$ interactions with mesons; however, s-wave kaon–pion interactions are weak due to chiral symmetry arguments and p-wave interactions such as $\pi + K \leftrightarrow K^*$ transitions are suppressed substantially by the approximately 'thermal' pion spectrum [37].

Furthermore, we have pursued the idea of [38, 39] that the $K^{\pm}$ spectra could be hardened by string–string interactions, which increase the effective string tension σ and thus the probability of producing mesons at high m_T [20, 39]. In order to estimate the largest possible effect of string–string interactions we have assumed that for two overlapping strings the string tension σ is increased by a factor of two, for three overlapping strings by a factor of three etc. Here the overlap of strings is defined geometrically assuming a transverse string radius R_s, which according to the studies in [40] should be $R_s \leq 0.25$ fm. On the basis of these assumptions (and $R_s = 0.25$ fm), we find only a small increase of the inverse slope parameters at AGS energies, where the string densities are low. At 160 A GeV the model gives a significant hardening of the spectra by about 15%, which, however, is still significantly less than the effect observed in the data.

Our findings are summarized in Fig. 4, where the dependence of the inverse slope parameter T (see Eq. (1)) on $\sqrt{s}$ is shown and compared to the experimental data [8, 41] for central Au + Au (Pb + Pb) collisions (l.h.s.) and pp reactions (r.h.s.). The upper and lower solid lines (with open circles) on the l.h.s. in Fig. 4 correspond to results from HSD calculations, where the upper and lower limits are due to fitting the slope T itself, an uncertainty in the repulsive $K^{\pm}$-pion potential or the possible effect of string overlaps. The slope parameters from pp collisions (r.h.s. in Fig. 4) are seen to increase smoothly with energy both in the experiment (full squares) and in the HSD calculations (full lines with open circles). The UrQMD results for pp collisions are shown as open triangles connected by the solid line and systematically lower than the slopes from HSD at all energies.

We mention that the RQMD model [38] gives higher inverse slope parameters for kaons at AGS and SPS energies than HSD and UrQMD, which essentially might be traced back to the implementation of effective resonances with masses above 2 GeV as well as 'color ropes' that decay isotropically in their rest frame [44]. A more detailed discussion of this issue is presented in [30].

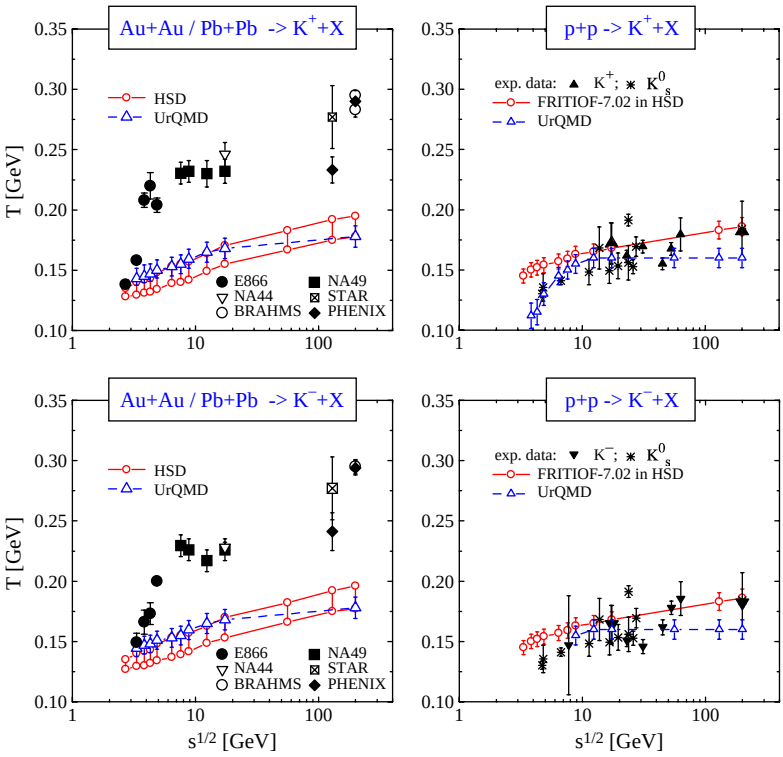

Fig. 4. Comparison of the inverse slope parameters T for K^+ and K^- mesons from central Au + Au (Pb + Pb) collisions (l.h.s.) and pp reactions (r.h.s.) as a function of the invariant energy $\sqrt{s}$ from HSD (upper and lower solid lines) and UrQMD (open triangles) with data from [8, 21, 27–29, 42] for AA and [29, 41, 43] for pp collisions. The upper and lower solid lines result from different limits of the HSD calculations as discussed in the text. The figure is taken from [30].

4. Thermodynamics in the T, μ_B plane

This still leaves us with the question of the origin of the rapid increase of the $K^\pm$ slopes with invariant energy for central Au + Au collisions at AGS energies and the constant slope at SPS energies (the 'step'), which is missed in both transport approaches. We recall that higher transverse particle momenta either arise from repulsive self-energies—in mean-field dynamics—or from collisions, which reduce longitudinal momenta in favor of transverse momenta [5, 45]. As shown above in Fig. 4, conventional hadron self-energy effects and hadronic binary collisions are insufficient to describe the dramatic increase of the $K^\pm$ slopes as a function of $\sqrt{s}$. This indicates additional mechanisms for the generation of pressure that is observed experimentally.

Here we propose that additional pre-hadronic/partonic degrees of freedom might be responsible for this effect already at ∼5 A GeV. Our arguments are based on a comparison of the thermodynamic parameters T and μ_B extracted from the transport models in the central overlap regime of Au + Au collisions [46] with the experimental

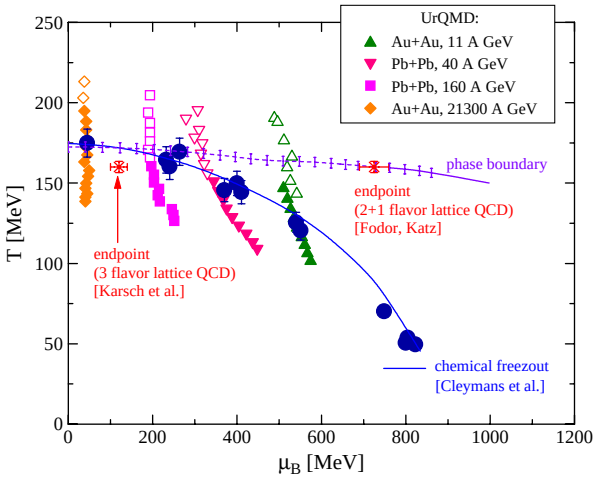

Fig. 5. The solid line characterizes the universal chemical freeze-out line from Cleymans et al. [47] whereas the full dots (with error bars) denote the 'experimental' chemical freeze-out parameters from [47]. The various symbols stand for temperatures T and chemical potentials μ_B extracted from UrQMD transport calculations for central Au + Au (Pb + Pb) collisions at 21.3 A TeV, 160, 40 and 11 A GeV [46] (see the text). The stars indicate the tricritical end-points from lattice QCD calculations by Karsch et al. [48] (left point) and Fodor and Katz [7] (right point). The horizontal line with error bars is the phase boundary from [7].

systematics on chemical freeze-out configurations [47] in the T, μ_B plane. The solid line in Fig. 5 characterizes the universal chemical freeze-out line from Cleymans et al. [47] whereas the full dots with error bars denote the 'experimental' chemical freeze-out parameters—determined from the fits to the experimental yields—taken from [47]. The various symbols (in vertical sequence) stand for temperatures T and chemical potentials μ_B extracted from UrQMD transport calculations for central Au + Au (Pb + Pb) collisions at 21.3 A TeV, 160, 40 and 11 A GeV [46] as a function of the reaction time (from top to bottom). The open symbols denote nonequilibrium configurations and correspond to T parameters extracted from the transverse momentum distributions, whereas the full symbols denote configurations in approximate pressure equilibrium in longitudinal and transverse direction.

During the nonequilibrium phase (open symbols) the transport calculations show much higher temperatures (or energy densities) than the 'experimental' chemical freeze-out configurations at all bombarding energies ($\geq$11 A GeV). These numbers are also higher than the tricritical end-points extracted from lattice QCD calculations by Karsch et al. [48] and Fodor and Katz [7] (stars with horizontal error bars). Though the QCD lattice calculations differ substantially in the value of μ_B for the critical end-point, the critical temperature T_c is in the range of 160 MeV in both calculations, while the energy density is in the order of 1 GeV/fm^3 or even below. Nevertheless, this diagram shows that at RHIC energies one encounters more likely a crossover between the different phases when stepping down in temperature during the expansion phase of the 'hot fireball'. This situation changes at lower SPS or AGS (as well as new GSI SIS-300) energies,

where for sufficiently large chemical potentials μ_B the crossover should change to a first-order transition [49], i.e., beyond the tricritical point in the (T, μ_B) plane. Nevertheless, Fig. 5 demonstrates that the transport calculations show temperatures (energy densities) well above the phase boundary (horizontal line with error bars) in the very early phase of the collisions, where hadronic interactions practically yield no pressure, but pre-hadronic degrees of freedom should do. This argument is in line with the studies on elliptic flow at RHIC energies—that is underestimated by 30% at mid-rapidity in the HSD approach for all centralities [31]. Only strong early stage pre-hadronic interactions might cure this problem.

5. Conclusions

Summarizing this survey, we point out that baryon stopping [50] and hadron production in central Au + Au (or Pb + Pb) collisions is quite well described in the independent transport approaches HSD and UrQMD. Also the 'longitudinal' rapidity distributions of protons, pions, kaons, antikaons and hyperons are similar in the two models and in reasonable agreement with available data. The exceptions are the pion rapidity spectra at the highest AGS energy and lower SPS energies, which are overestimated by both models [17]. As a consequence, the HSD and UrQMD transport approaches underestimate the experimental maximum of the K^+/π^+ ratio ('horn') at ~20 to 30 A GeV. However, we point out that the maxima in the K^+/π^+ and $(\Lambda + \Sigma^0)/\pi$ ratios dominantly reflect a change from baryon to meson dominated dynamics with increasing bombarding energy.

We have found that the inverse slope parameters T for $K^\pm$ mesons from the HSD and UrQMD transport models are practically independent of system size from pp up to central Pb + Pb collisions and show only a slight increase with collision energy, but no 'step' in the $K^\pm$ transverse momentum slopes. The rapid increase of the inverse slope parameters of kaons for collisions of heavy nuclei (Au + Au) found experimentally in the AGS energy range, however, is not reproduced by either model (see Fig. 4). Since the pion transverse mass spectra—which are hardly affected by collective flow—are described sufficiently well at all bombarding energies [30], the failure has to be attributed to a lack of pressure. We have argued—based on lattice QCD calculations at finite temperature and baryon chemical potential μ_B [7, 48] as well as the experimental systematics in the chemical freeze-out parameters [47]—that this additional pressure should be generated in the early phase of the collision, where the 'transverse' energy densities in the transport approaches are higher than the critical energy densities for a phase transition (or crossover) to the QGP. The interesting finding of our analysis is that pre-hadronic degrees of freedom might already play a substantial role in central Au + Au collisions at AGS energies above ~5 A GeV.

We recall that the systematic studies of in-plane and elliptic proton flow in Au + Au collisions at AGS energies [51–53] also indicate a 'softening' of the nuclear equation of state (EoS) at 4–6 A GeV, which further supports our present findings.

Acknowledgements

This paper was supported by DFG, GSI, BMBF and DESY.

References

[1] J. Rafelski, B. Müller, Phys. Rev. Lett. 48 (1982) 1066.
[2] J.D. Bjorken, Phys. Rev. D 27 (1983) 140.
[3] H.H. Gutbrod, J. Aichelin, K. Werner, Quark Matter 2002; Nuclear Phys. A 715 (2003) 1.
[4] F. Karsch et al., Nuclear Phys. B 502 (2001) 321.
[5] H. Stöcker, W. Greiner, Phys. Rep. 137 (1986) 277.
[6] W. Cassing, E.L. Bratkovskaya, S. Juchem, Nuclear Phys. A 674 (2000) 249.
[7] Z. Fodor, S.D. Katz, JHEP 0203 (2002) 014.
[8] V. Friese et al., NA49 Collaboration, J. Phys. G 30 (2004) 119.
[9] M.I. Gorenstein, M. Gaździcki, K. Bugaev, Phys. Lett. B 567 (2003) 175.
[10] M. Gaździcki, M.I. Gorenstein, Acta Phys. Polon. B 30 (1999) 2705.
[11] M. Gaździcki, J. Phys. G 30 (2004) 161.
[12] L. Van Hove, Phys. Lett. B 118 (1982) 138.
[13] S.A. Bass et al., Prog. Part. Nuclear Phys. 42 (1998) 255.
[14] M. Bleicher et al., J. Phys. G 25 (1999) 1859.
[15] J. Geiss, W. Cassing, C. Greiner, Nuclear Phys. A 644 (1998) 107.
[16] W. Cassing, E.L. Bratkovskaya, Phys. Rep. 308 (1999) 65.
[17] H. Weber, E.L. Bratkovskaya, W. Cassing, H. Stöcker, Phys. Rev. C 67 (2003) 014904.
[18] K. Hagiwara et al., Phys. Rev. D 66 (2002) 010001 (Review of Particle Properties).
[19] B. Andersson et al., Z. Phys. C 57 (1993) 485.
[20] Z.W. Lin et al., Nuclear Phys. A 698 (2002) 375.
[21] L. Ahle et al., E866 and E917 Collaboration, Phys. Lett. B 476 (2000) 1;
L. Ahle et al., E866 and E917 Collaboration, Phys. Lett. B 490 (2000) 53.
[22] J. Klay et al., E895 Collaboration, Phys. Rev. C 68 (2003) 054905.
[23] S. Ahmad et al., E891 Collaboration, Phys. Lett. B 382 (1996) 35;
C. Pinkenburg et al., E866 Collaboration, Nuclear Phys. A 698 (2002) 495c.
[24] S.V. Afanasiev et al., NA49 Collaboration, Phys. Rev. C 66 (2002) 054902.
[25] A. Mischke et al., NA49 Collaboration, J. Phys. G 28 (2002) 1761; Nuclear Phys. A 715 (2003) 453.
[26] F. Antinori et al., WA97 Collaboration, Nuclear Phys. A 661 (1999) 130c.
[27] D. Ouerdane et al., BRAHMS Collaboration, Nuclear Phys. A 715 (2003) 478;
J.H. Lee et al., J. Phys. G 30 (2004) 85.
[28] S.S. Adler et al., PHENIX Collaboration, preprint nucl-ex/0307010; preprint nucl-ex/0307022.
[29] C. Adler et al., STAR Collaboration, preprint nucl-ex/0206008;
O. Barannikova et al., Nuclear Phys. A 715 (2003) 458;
K. Filimonov et al., preprint hep-ex/0306056.
[30] E.L. Bratkovskaya et al., preprint nucl-th/0402026.
[31] E.L. Bratkovskaya, W. Cassing, H. Stöcker, Phys. Rev. C 67 (2003) 054905.
[32] W. Cassing, K. Gallmeister, E.L. Bratkovskaya, C. Greiner, H. Stöcker, Prog. Part. Nucl. Phys. doi:10.1016/j.ppnp.2004.02.006.
[33] S. Soff et al., Phys. Lett. B 551 (2003) 115.
[34] K. Redlich, J. Cleymans, H. Oeschler, A. Tounsi, Acta Phys. Polon. B 33 (2002) 1609.
[35] E.L. Bratkovskaya, S. Soff, H. Stöcker, M. van Leeuwen, W. Cassing, Phys. Rev. Lett. 92 (2004) 032302. Preprint nucl-th/0307098.
[36] A. Förster et al., KaoS Collaboration, J. Phys. G 28 (2002) 2011.
[37] B.V. Martemyanov et al., nucl-th/0212064.
[38] H. Sorge, Phys. Rev. C 52 (1995) 3291.
[39] S. Soff et al., Phys. Lett. B 471 (1999) 89.
[40] J. Geiss et al., Phys. Lett. B 447 (1999) 31.
[41] I. Kraus et al., NA49 Collaboration, J. Phys. G 30 (2004).
[42] I.G. Bearden et al., NA44 Collaboration, preprint nucl-ex/0202019.
[43] M. Kliemant, B. Lungwitz, M. Gaździcki, preprint hep-ex/0308002.
[44] H. van Hecke et al., Phys. Rev. Lett. 81 (1998) 5764.
[45] W. Cassing, U. Mosel, Prog. Part. Nuclear Phys. 25 (1990) 235.
[46] L.V. Bravina et al., Phys. Rev. C 60 (1999) 024904; Nuclear Phys. A 698 (2002) 383.

[47] J. Cleymans, K. Redlich, Phys. Rev. C 60 (1999) 054908.
[48] F. Karsch et al., preprint hep-lat/0309116.
[49] E. Shuryak, Prog. Part. Nucl. Phys. doi:10.1016/j.ppnp.2004.02.025.
[50] H. Weber, E.L. Bratkovskaya, H. Stöcker, Phys. Lett. B 545 (2002) 285.
[51] P. Danielewicz et al., Phys. Rev. Lett. 81 (1998) 2438.
[52] P.K. Sahu, W. Cassing, Nuclear Phys. A 712 (2002) 357.
[53] E.G. Nikonov, A.A. Shanenko, V.D. Toneev, Heavy Ion Phys. 8 (1998) 89.